PHYSICAL REVIEW B VOLUME 37, NUMBER 6 15 FEBRUARY 1988-II

Interstitial migration of hydrogen and helium in platinum

R. Vassen and P. Jung
Institut für Festkörperforschung, Kernforschungsanlage Jülich, D-5170 Jülich, West Germany
(Received 15 June 1987)

Hydrogen and helium were implanted with energies from 0.25 to 3.0 keV into 0.1-μm Pt films at 4.2 K. Resistivity damage rates were measured and subsequent isochronal annealing was performed up to 400 K. From damage rates at energies below the threshold for Frenkel-pair production, the resistivity change per implanted atom was derived, giving $\rho_H = 0.5\ \mu\Omega\,cm/at.\,\%$ and $\rho_{He} = 5\ \mu\Omega\,cm/at.\,\%$, respectively. Damage rate measurement of deuterium slightly above threshold indicated that molecular hydrogen contributes to defect production. Resistivity recovery after helium implantation started around 17 K and showed close similarity to Frenkel-pair recovery. This result is explained by the onset of mobility of the He atoms at this temperature. After hydrogen implantation above threshold mainly Frenkel-pair recovery was observed while implantation below threshold gave a large recovery step around 50 K, indicating hydrogen mobility at this temperature.

I. INTRODUCTION

The presence of relatively small amounts of hydrogen or helium can cause embrittlement in metallic materials. This is mostly due to their diffusion to, and subsequent agglomeration at, dislocations or grain boundaries. Theoretical work on interstitial helium and hydrogen in fcc metals indicates mobility well below room temperature.[1] In a metal of low solubility for both H and He such as platinum the only possible way to investigate interstitial diffusion of these gases is implantation at low temperatures with energies below the threshold for atomic displacement. This is necessary to prevent the production of Frenkel pairs (vacancy plus interstitial), as vacancies would strongly trap the gas atoms. The experiments were performed on platinum because the ranges of H and He at the threshold energy are larger in heavy elements than in lighter elements (Fig. 1). Nevertheless thin films ($\simeq 100$ nm) were used to obtain sufficient resolution in the electrical resistivity measurement, which was used as a convenient and sensitive method during implantation as well as during the subsequent isochronal annealing.

It can be shown[5] that the implantation profile (see Appendix) does not influence the resistivity change $\Delta\rho$ as long as the residual resistance ρ_0 is large compared to $\Delta\rho$. For the present specimens and the implantation doses used the relative resistance change $\Delta R/R_0$ always approximated closely the relative resistivity change $\Delta\rho_{hom}/\rho_0$ which would have been observed for homogeneous implantation.

II. EXPERIMENTAL DETAILS

The platinum films were prepared by evaporating 99.999% platinum on sapphire at 350 °C in a vacuum of 10^{-6} mbar. Stainless steel masks on the substrate produced gauge sections of the four wire resistance specimens, 6 mm long and 1.5 mm wide. Afterwards the specimens were annealed for 1 h at 1023 K. Thicknesses from 90 to 310 nm were used; the residual-to-room-temperature resistivity ratio was about 12. With measuring currents between 20 and 30 mA and a voltage sensitivity of 100 nV resistivity changes of $\approx 10^{-13}\ \Omega\,m$ could be measured.

The specimens were mounted on the cold head of an evaporation cryostat which could be heated to temperatures from 5 to 400 K. The temperature was measured with Au-Fe-Ni-Cr and copper-Constantan thermocouples.

The implantation was performed with a conventional small ion source with energies adjustable from 0.25 to 3.0 keV, giving maximum fluxes at these energies of 10^{10} and 5×10^{11} particles/(cm^2 s), respectively. Two different

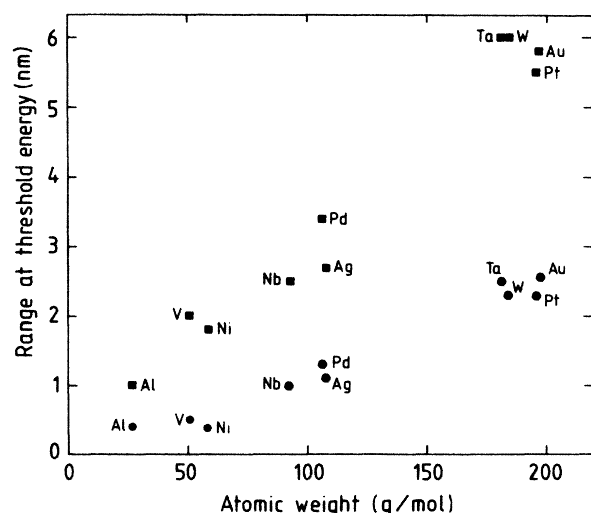

FIG. 1. Ranges of helium (●) and hydrogen (■) for implantation at the threshold energy for atomic displacement (Refs. 2–4).

©1988 The American Physical Society

isochronal annealing schedules were used, raising the temperature in logarithmic steps of $\Delta T/T=0.13$ and 0.33, respectively. Holding times at temperature were 600 s and cooling rates ranged from 0.5 K/s for $T\geq 100$ K to 5 K/s for $T\leq 20$ K. The apparatus is described in more detail elsewhere.[6]

III. RESULTS

A. Helium in platinum

1. Damage rates

The electrical resistivity change during implantation is comprised of contributions of the implanted atoms, e.g., hydrogen or helium, and of the lattice defects produced:

$$\Delta\rho=\rho_{\mathrm{He,H}}\frac{N_{\mathrm{He,H}}}{N_0}+\rho_F\frac{N_F}{N_0} . \quad (1)$$

$\rho_{\mathrm{He,H}}$ and ρ_F are the resistivity contributions per unit concentration of implanted helium or hydrogen atoms and of Frenkel pairs and $N_{\mathrm{He,H}}$, N_F, and N_0 are the numbers of He or H, Frenkel pairs, and target atoms, respectively. The damage rate is obtained by dividing $\Delta\rho$ by the particle dose $\Delta\phi=N_{\mathrm{He,H}}(d/V)$ where d and V are target thickness and volume, respectively.

$$\frac{\Delta\rho}{\Delta\phi}\frac{n_0 d}{\rho_F}=\frac{\rho_{\mathrm{He,H}}}{\rho_F}+\frac{N_F}{N_{\mathrm{He,H}}} , \quad (2)$$

where $n_0=N_0/V$ is the atomic density of the target. $\rho_{\mathrm{He,H}}/\rho_F$ is an energy-independent quantity which stems from the "pure" implantation while the second term gives the number of defects produced per implanted atom.

The open circles (○) in Fig. 2 give the above normalized damage rates measured during implantation of He^+ into platinum. The measured dose values $\Delta\phi_m$ were corrected for backscattering by using the TRIM code (see Appendix). With the backscattering coefficient (r) the correction factors $\Delta\phi/\Delta\phi_m=(1-r)$ range from 0.36 at 0.25 keV He^+ to 0.45 at 3.0 keV He^+ implantation. Backscattering of charged ions was neglected.[7] Approximate corrections for secondary electron (SE) emission were used by taking mean SE coefficients (γ) given for molybdenum and tungsten in Ref. 8. These SE correction factors $1/1+\gamma$ varied from 0.80 to 0.69 at 0.25 and 3.0 keV, respectively. The total correction factor $(1-r)/(1+\gamma)$ shows only a negligible energy dependence from 0.29 (0.25 keV) to 0.31 (3.00 keV) with an intermediate maximum of 0.33 at 0.8 keV. The data points in Fig. 2 level off at energies below about 0.6 keV at a value of about 0.48 for $\rho_{\mathrm{He}}/\rho_F$ according to Eq. (2). Inserting $\rho_F=10$ $\mu\Omega$ cm/at. %[4] gives a value of 4.8 $\mu\Omega$ cm/at. % for ρ_{He}. The data points at 0.25 keV are at variance with these results. This may be caused by errors of beam current measurement at this low energy resulting from space charges or by surface contamination.

When $\rho_{\mathrm{He}}/\rho_F$ is subtracted from the data, the solid circles (●) are obtained, representing the number of

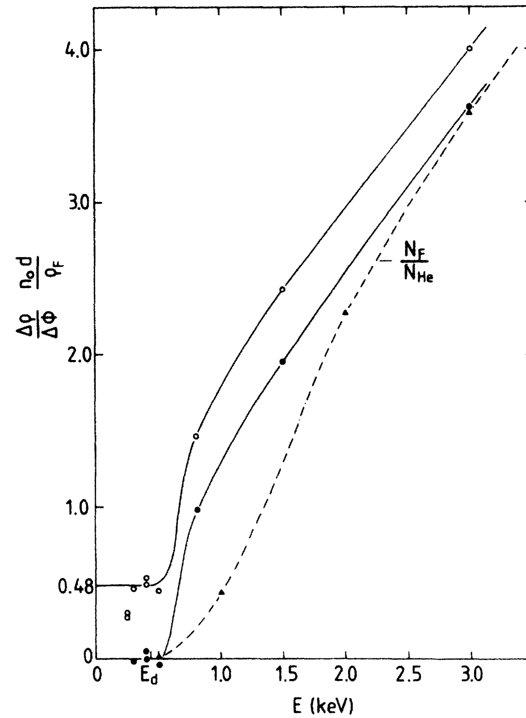

FIG. 2. Normalized damage rates of helium in platinum (○) and the number of produced Frenkel pairs per implanted helium atom (●, experimental; —·▲–, calculated).

Frenkel pairs produced per implanted ion N_F/N_{He}. It is possible to calculate this quantity from electron damage rate data by using the known scattering cross sections for electrons and light ions.[4] These calculations are given by the solid triangles (▲) and the dash-dotted line (—·—·—·), obviously in good agreement with the solid circles with respect to the threshold energy and to the absolute values at higher energies, but deviating at intermediate energies.

2. Recovery

Figure 3 shows the resistivity recovery after helium implantation in platinum. The remaining resistance change ($R-R_0$) after each annealing step is normalized to the resistivity change after implantation (R_i-R_0). Included is a control measurement of an unimplanted specimen with an arbitrary normalization to R_i-R_0 $=0.24$ mΩ, corresponding to the lowest implantation dose used. Two recovery curves after 3-MeV-electron and fast-neutron irradiation are also shown.[9,10] The maximum energy transferred by 3-MeV electrons is equal to that of 1.65-keV helium ions.

The mean helium concentrations ($\bar{c}_{\mathrm{He}}$) were calculated from the total resistivity change $\Delta\rho$ during implantation, with the normalized implantation profile $f(x)$ obtained from the TRIM code and using the damage rates of Fig. 2 and $\rho_F=10$ $\mu\Omega$ cm/at. %.[4]

The equation used was

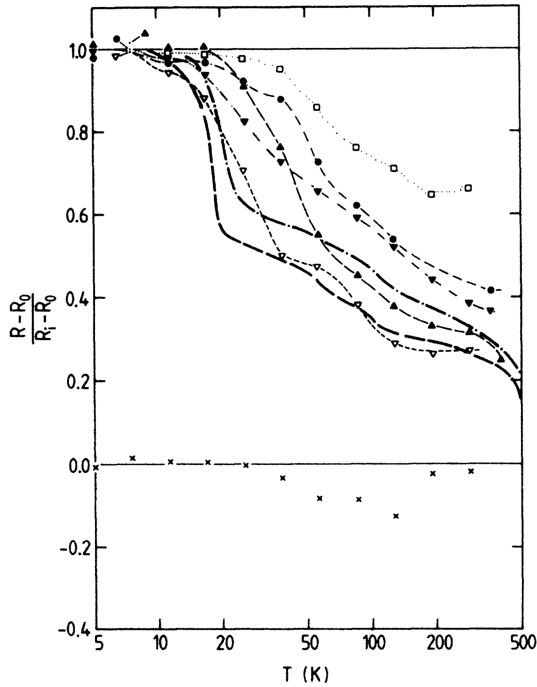

FIG. 3. Resistivity recover of platinum after helium implantation of various energies E (keV) and doses $\bar{c}_{\rm He}$ (ppm): ●, $E=0.25$, $\bar{c}_{\rm He}=117$; ▲, $E=0.25$, $\bar{c}_{\rm He}=70$; □, $E=0.42$, $\bar{c}_{\rm He}=390$; ▼, $E=1.65$, $\bar{c}_{\rm He}=64$; ▽, $E=1.65$, $\bar{c}_{\rm He}=1.2$. Also recoveries after 3-MeV-electron irradiation (— — —, Ref. 9) and fast neutron irradiation (—·—·—·, Ref. 10) and a control measurement (×) are given.

$$\bar{c}_{\rm He}=\frac{\Delta\phi}{n_0 d}\int_0^d f^2(x)dx=\frac{\Delta\rho}{\left[\dfrac{\Delta\rho}{\Delta\phi}\dfrac{n_0 d}{\rho_F}\right]\rho_F}\int_0^d f^2(x)dx \; . \tag{3}$$

Figure 4 is obtained when damage rates are measured as a function of implantation temperature. In this type of experiment the instantaneous concentration of mobile defects (e.g., He atoms) should be low, reducing the probability of clustering.

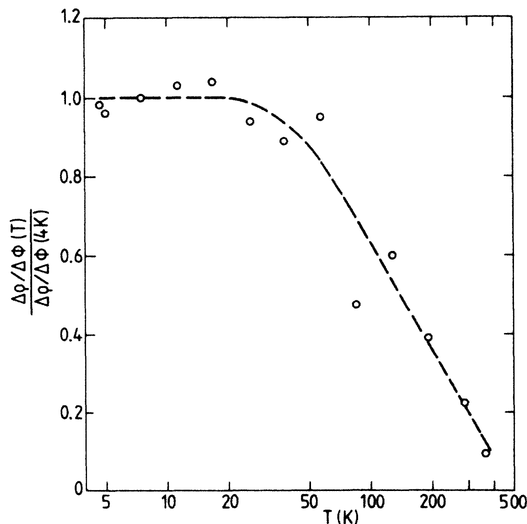

FIG. 4. Normalized damage rates for 0.4-keV He^+ in platinum as a function of implantation temperature.

B. Hydrogen in platinum

1. Damage rates

The open circles (○) in Fig. 5 show normalized damage rates of D_2^+ on platinum as a function of the implantation energy, while for H_2^+ up to 3.0 keV no energy dependence of the damage rates was observed. The energies $E(D_2)$ are related to the D_2^+ particles used for implantation, while $\Delta\phi$ is the dose of the individual D atoms.

Corrections for backscattering by using the TRIM code gave correction factors which varied from 0.30 for 0.4 keV to 0.52 for 3.0 keV. The secondary electron emission coefficients were calculated by extrapolating values for gold[8] down to low energies, giving correction factors from 0.63 to 0.38 at 0.4 and 3.0 keV. The total correction factors ranged from 0.19 (0.25 keV) to 0.20 (3.0 keV).

The damage rates level off at low energies at a value of $\rho_H/\rho_F=0.052$ according to Eq. (2). Taking $\rho_F=10$ $\mu\Omega$ cm/at. % (Ref. 4) for ρ_H a value of 0.5 $\mu\Omega$ cm/at. % is obtained. If ρ_H/ρ_F is subtracted from the data, the solid circles, representing $N_F/N_{\rm D}$ are obtained. As for He, the defect production per implanted atom can also be calculated from electron damage rates. Two assumptions are possible. If a D_2 molecule is the damaging unit, the upper curve is obtained. On the other hand if the D_2 molecule splits at the surface and individual D atoms of energy $E/2$ interact with the target atoms, then the lower curve is obtained. The measured defect production (●) takes off at a threshold energy in close

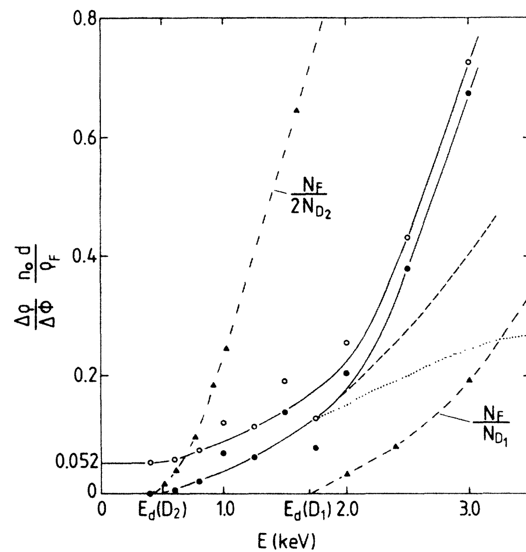

FIG. 5. Normalized damage rates of deuterium in platinum (–○–) and the number of produced Frenkel pairs per implanted deuterium atom (–●–, experimental; –▲··– and –▲·–, calculated). Dashed and dotted lines are explained in the text.

agreement with the calculated curve for D_2^+ damage, but with a lower ascent.

2. Recovery

Figure 6 shows the recovery of Pt after hydrogen implantation at various energies. The mean concentrations ($\bar{c}_H$) were calculated according to Eq. (3) from the resistivity increases and the calculated (TRIM code) implantation profiles and using the damage rates of Fig. 5. All curves in Fig. 6 show two recovery steps in the temperature region between 40 and 130 K. Included are recovery curves after 3-MeV-electron and fast-neutron irradiation. The reference measurement on an unimplanted specimen (x) is normalized to $R_i - R_0 = 0.59$ mΩ corresponding to the lowest implantation dose used. The dotted line (· · · ·) indicates a calculated recovery curve for diffusion of the hydrogen atoms to the surface with a diffusion coefficient[11]

$$D\ (\mathrm{cm^2/s}) = 6.2\times10^{-3}\ \exp\left[\frac{-0.12\ \mathrm{eV}}{kT}\right].$$

Figure 7 shows recovery curves for smaller temperature steps between 38 and 128 K. The two recovery steps of Fig. 6 can be resolved into three steps centered around 47, 80, and 110 K. In Fig. 7 a recovery curve after 3-keV D_2^+ implantation is also included. This curve falls close to the recovery curve after 3-MeV-electron irradiation.

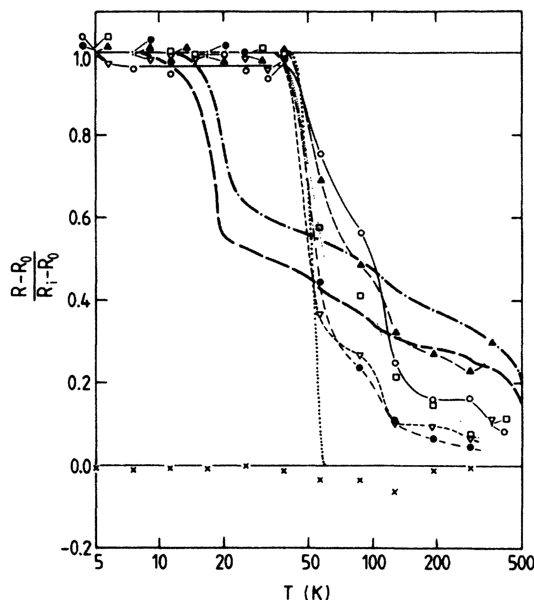

FIG. 6. Resistivity recoveries of platinum after hydrogen implantation of various energies E (keV) and doses $\bar{c}_{H,D}$ (ppm) H: ●, $E=0.4$, $\bar{c}_H=410$; ▲, $E=0.4$, $\bar{c}_H=2140$; □, $E=0.98$, $\bar{c}_H=1280$; ∇, $E=3.0$, $\bar{c}_H=490$. D: ○, $E=0.4$, $\bar{c}_H=1870$. For comparison recoveries after 3-MeV-electron irradiation (— — —, Ref. 9) and fast-neutron irradiation (—·—·—·, Ref. 10), control measurement (×) and calculated recovery with D $(\mathrm{cm^2/s}) = 6.2\times10^{-3}\exp(-0.12/kT)$ (· · · ·) are included.

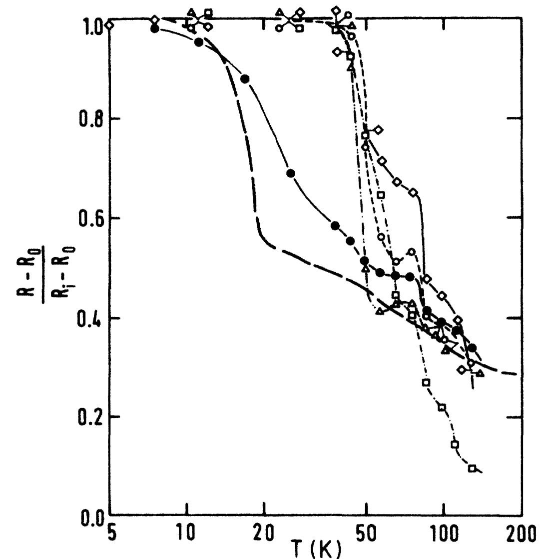

FIG. 7. Resistivity recoveries of platinum after hydrogen implantation at various energies E (keV) and doses $\bar{c}_{H,D}$ (ppm) H: □, $E=0.4$, $\bar{c}_H=980$; △, $E=3.0$, $\bar{c}_H=170$; ○, $E=3.0$, $\bar{c}_H=880$. D: ◇, $E=0.4$, $\bar{c}_H=590$; ●, $E=3.0$, $\bar{c}_H=10$. For comparison a recovery after 3-MeV-electron irradiation (— — —, Ref. 9) is shown.

IV. DISCUSSION

A. Damage rate curves

The resistivity values per unit concentration of hydrogen or helium derived from the low-energy part of the damage rate curves in Figs. 2 and 5 can be compared to resistivity contributions (in μΩm) of other imperfections in metals of the Pt group (Table I).

A value of 4.2 μΩ m was observed for room-temperature implantation of helium in nickel.[16] At this temperature the interstitial helium and the simultaneously produced interstitials are mobile. The final state therefore will consist of substitutional He atoms, i.e., He atoms trapped in a vacancy, and dislocation loops which contribute negligibly to the electrical resistivity. This would mean that the resistivity contributions of vacancies, self-interstitials, interstitial He and substitutional

TABLE I. Resistivity contributions (in μΩ m) of imperfections in metals of the Pt group.

	Pt	Pd	Ni
Vacancy	5.8[a]		
Frenkel pair	10.0[b]	9.0[b]	7.0[b]
Hydrogen	0.5	0.65[c]	0.67[c]
Helium	4.8		
Carbon		3.1[d]	3.3[e]

[a]Reference 12.
[b]Reference 4.
[c]Reference 13.
[d]Reference 14.
[e]Reference 15.

He in these metals are all of about the same magnitude.

The damage rate curves in Figs. 2 and 5 take off exactly at the threshold for atomic displacement in Pt of 34 eV.[4] The shape of the measured helium defect production rates (●) appreciably exceeds the N_F/N_{He} curve derived from electron irradiation. Only above 2.0 keV ($\simeq 4E_d$) do both curves close up.

For deuterium two curves can be calculated, representing defect production by D atoms (N_F/N_{D_1}) or by D pairs ($N_F/2N_{D_2}$). Both curves are related by

$$\frac{N_F}{N_{D_1}}(E)=\frac{N_F}{N_{D_2}}(E/4) . \tag{4}$$

The threshold of the measured curve clearly indicates defect production by pairs. But in Fig. 5 the measured defect production rates (●) take off much slower than the $N_F/2N_{D_2}$ curve calculated from the electron data. Actually, for energies from $E_d(D_2)$ to $E_d(D_1)$, the measured values are consistently lower than the calculated curve by a factor of about 0.16. The measured production rate per D atom $\overline{N_F}/N_D$ can be expressed by the contributions from atomic (D_1) and molecular deuterium (D_2) by

$$\frac{\overline{N_F}}{N_D}=\frac{N_F}{N_{D_1}}\frac{N_{D_1}}{N_D}+\frac{N_F}{2N_{D_2}}\frac{2N_{D_2}}{N_D} . \tag{5}$$

For $E<E_d(D_1)$, $N_F/N_{D_1}=0$ and $(\overline{N_F}/N_D)/(N_F/2N_{D_2})=0.16$, giving $2N_{D_2}/N_D=0.16$. That means that about 16% of the original D_2^+ particles interact as a "molecule" with the target atoms. Assuming continuing energy independence of this fraction the dotted line in Fig. 5 is obtained. Insertion in Eq. (5) with $N_{D_1}+2N_{D_2}=N_D$ yields for $E>E_d(D_1)$

$$\frac{\overline{N_F}}{N_D}=\frac{N_F}{N_{D_1}}\times 0.84+\frac{N_F}{2N_{D_2}}\times 0.16 ,$$

giving the dashed line in Fig. 5.

In Fig. 5, the second term of this expression is given by the dotted line, while the dashed line gives the sum of both terms. Obviously, measured defect production rates exceed the calculated values in the near-threshold region considerably, but less than in the case of He (Fig. 2). This discrepancy is beyond the experimental error of both the electron and the present light-ion damage rates. Possible reasons may be errors in the correction factors for backscattering or in the scattering cross sections used.

If we now transfer the results derived from deuterium implantation to hydrogen, we would expect the threshold energy at about 0.85 keV for H_2^+ (3.35 keV for H_1^+) according to the lower mass of the light isotope. However, no energy dependence of the damage rate is observed up to 3.0 keV. That means that hydrogen transfers its energy only as a single atom and not as a H_2^+ molecule. Possible reasons are the higher velocities of the H_2^+ molecules compared to the D_2^+ molecules or the lower mass of the H atoms, which perhaps leads to a quicker repulsion of the two hydrogen atoms in the metal.[17]

Studies on cascade production by energetic atom pairs versus single atoms using transmission electron microscopy[18] and sputtering[19] showed significant effects of cascade overlap but are probably not affected by the present effects in the near-threshold region.

B. Recovery

The damage rate data (Fig. 2) allow us to separate the resistivity contributions of implanted helium and Frenkel defects: In Fig. 3 the resistivity of the 0.25- and 0.42-keV curves thus stems entirely from implanted He, while the Frenkel pairs cause more than 80% of the resistivity during 1.65-keV implantation. In this case especially the low-dose curve (∇) is in fair agreement with the recovery curve after electron irradiation, while at the higher dose recovery is reduced due to enhanced agglomeration of defects. While annealing of Frenkel pairs in platinum starts around 10 K, recovery of the low-energy implanted specimens begins only around 17 K. The slope of the He recovery curve increases with decreasing dose, but even at the lowest attainable dose, the slope is still much less steep than expected for first- or second-order reactions or for free diffusion. We therefore have to recognize that due to the still rather high He concentration, a series of clustering reactions occurs when the helium atoms start to migrate. The decrease in resistivity is then due to the reduced resistivity contribution of helium atoms in larger clusters and possibly to some extent due to losses to the surface. If free diffusion of helium to the surface is considered, starting from the implantation profile derived from the TRIM code and using a typical prefactor $D_0=0.1$ cm²/s (Ref. 20), the initial part of the recovery curve is matched for a migration enthalpy $H_{He}^m=0.08$ eV. If it is presumed that resistivity annealing is caused by clustering an insignificantly higher H_{He}^m value is obtained. For higher He concentrations the recovery is more gradual, especially up to about 40 K; at higher temperatures much less recovery is observed. This may be due to a reduced fraction of helium reaching the surface or due to a larger fraction of smaller clusters, as nucleation is enhanced in the more concentrated specimens.

The similarity of the recovery after He^+ implantation and after electron irradiation may suggest a different interpretation in terms of self-interstitial atoms (SIA's) which could be produced by self-trapping[21] of He atoms. In this case one would have to assume He mobility already during implantation at 4.2 K and nucleation of He bubbles which finally grow by emitting SIA's. During growth the resistivity would then increase due to the formation of SIA's (ρ_{SIA}) while the contribution from He in the bubbles (ρ'_{He}) decreases. Eventually when all He ends up in large bubbles ($\rho'_{He}\approx 0$) the resistivity change caused by a unit concentration of implanted He atoms would become

$$\rho_{He}\approx \nu\rho_{SIA} , \tag{2'}$$

where ν is the estimated number of SIA's emitted per He

atom in the bubbles, estimated at about 0.5 for fcc Ni.[21] According to Ref. 21 SIA emission starts at a bubble size of about 5 He atoms. The present damage rates at low energies would give $\nu=1.1$ if $\rho_{\rm SIA}=0.42\rho_F$ is taken from a comparison of Frenkel pair[4] and vacancy[12] resistivities in platinum. On the other hand there are reservations against this interpretation.

In order to trap mobile helium atoms effectively and grow, the mutual distance of bubbles has to be smaller than their average distance to the surface. This sets a lower limit to the bubble concentration of about $c_b \geq (a_0/d)^3 \approx 1.8\times10^{-4}$, where a_0 denotes atomic distance (0.28 nm) and d denotes implantation depth (≈ 5 nm). According to Ref. 21, SIA emission begins only above 5 atoms per bubbles, setting a lower limit to the He concentration of about $5c_b \approx 10^{-3}$. This value is above the concentrations used in the present experiment (Fig. 3).

If nevertheless SIA emission would have started within the present He concentration range, some change in damage rate (resistivity change per dose) should have been expected. But a constant damage rate was observed for all energies within the experimental accuracy.

Resistivity recovery after hydrogen and deuterium implantation shows a dominating step around 47 K (Fig. 6). Diffusion to the surface would yield an activation enthalpy $H^m_{\rm H,D}=0.12$ eV for a prefactor of the diffusion coefficient $D_0=6.2\times10^{-3}$ cm^2/s, derived from high-temperature measurements.[11] This step is in agreement with results from channeling experiments in platinum[22] where around 50 K a transition of deuterium atoms from octahedral to tetrahedral interstitial sites was observed. This transition may comprise short-range diffusion to implantation-induced lattice defects.

To discriminate between recovery by losses to the surface and by agglomeration, the average concentration and the spatial distribution were varied by using different doses and different implantation energies, i.e., particle ranges, respectively. This is shown in Fig. 7 where smaller temperature increments are used. The 0.4-keV, 980-ppm (□) and the 3.0-keV, 880-ppm (○) curves of H, which have different depth distributions but similar average concentrations, show similar behavior within the first step. This indicates that losses to the surface are of minor importance. On the other hand by comparing the two 3.0-keV H curves with different concentrations (△,○) somewhat increased recovery is observed in the less-concentrated specimen, emphasizing some effect of agglomeration. From the present experiments it cannot be safely decided whether the resistivity

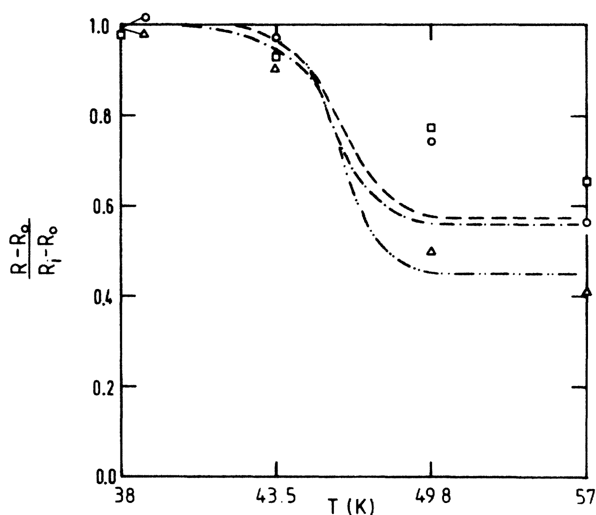

FIG. 8. Calculation of hydrogen recoveries with different initial profiles [corresponding to implantation energy E (keV) and concentrations $\bar{c}_{\rm H}$ (ppm); see text]. $E=0.4$, $\bar{c}_{\rm H}=980$: □, experimental; —·—·—·, theoretical. $E=3.0$, $\bar{c}_{\rm H}=880$: ○, experimental; — — —, theoretical. $E=3.0$, $\bar{c}_{\rm H}=170$: △, experimental; –···–, theoretical.

retained above the 47-K stage is entirely due to agglomeration, or if trapping of helium at impurity atoms is also important. The fact that two more recovery stages are observed is one hint that two different processes may be involved. A more quantitative analysis was done by using a numerical model. The model simulated the diffusion of hydrogen atoms starting with their initial distribution given by the TRIM profile and allowing for clustering and trapping at impurities. The following parameters were used. The trap concentration was about 0.2 at. % derived from the residual resistivity ($\simeq 1$ μΩ cm) divided by a specific resistivity per impurity of 5 μΩ cm/at. %. It was assumed that the resistivity per hydrogen atom does not change during clustering. The experimental data are then best fit by the calculations (Fig. 8) if it is assumed that by trapping the resistivity per hydrogen atom is reduced to 40% of its original value.

Figure 7 also contains two recovery curves after deuterium implantation. As already mentioned the upper part of the 3.0-keV curve agrees fairly well with the recovery after electron irradiation. The damage rate curves show that about 93% of the resistivity increase in this case is due to Frenkel pair formation while only

TABLE II. TRIM results of low-energy hydrogen and helium implantation in platinum.

Ion	Energy (keV)	Mean implantation depth (nm)	Backscattering factor	$N_F/N_{\rm ion}$
H_2^+	0.4	2.94	0.734	
H_2^+	3.0	10.8	0.510	
D_2^+	0.4	3.43	0.690	
He^+	0.25	3.43	0.644	
He^+	1.65	10.9	0.576	2.6

about 7% results from the implanted hydrogen. Nevertheless the three stages observed after subthreshold implantation are also clearly observed, especially the one at 80 K. The recovery after 0.4-keV deuterium implantation is smaller than after hydrogen implantation at comparable doses. A tentative explanation is possible if one considers the effect of ion mass on slowing down the implanted particles in the target. The implanted H_2^+ or D_2^+ molecules will then lose their binding electron within a few atomic layers.[23] Then a repulsion of the screened H or D atoms starts[17] which leads to separation of the two atoms, even without scattering by the target atoms. For equal repulsive force the separation is faster for the lighter H atoms than for the D atoms. Thus it is possible that the deuterium atoms come to rest closer to each other, thereby increasing the possibility for reclustering upon becoming mobile.

Beside the main step at 47 K there is another one at about 80 K. The step height is nearly proportional to the concentration and thus may be tentatively ascribed to the dissociation of hydrogen clusters. From the temperature of this step an activation energy of about 0.2 eV can be estimated for a dissociation reaction. Subtracting the migration energy (0.12 eV) results in a binding energy of H atoms in the cluster of about 0.08 eV. This is of the same order of magnitude as the H-H binding energy in Nb (0.065 eV).[24] Then the last measured step at 110 K may be ascribed to the dissociation of H atoms from impurities with an estimated dissociation energy of 0.28 eV, corresponding to a binding energy of about 0.16 eV. The decrease in resistivity in this later step can be due to diffusion of H out of the gauge section or due to escaping through the surface.

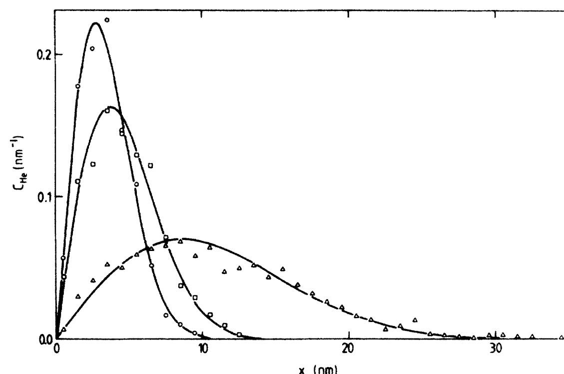

FIG. 9. Implantation profiles of helium in platinum calculated with the TRIM code for 0.25 keV (○), 0.42 keV (□), and 1.65 keV (△).

APPENDIX: THE TRIM PROGRAM

The TRIM program is the most commonly used Monte Carlo simulation method for the calculation of range profiles, backscattering, and damage rates of implanted ions. The TRIM version published in Ref. 25 was the one used. Some characteristic parameters of the TRIM results are stated in Table II and in Fig. 9.

ACKNOWLEDGMENT

The authors are deeply indebted to K. Reichelt, M. Rey and F. Römer for preparing the film specimens. The "Institut für Festkörperforschung" is affiliated with "Association Euratom—KFA."

[1]M. I. Baskes and C. F. Melius, Phys. Rev. B **20**,8 3197 (1979).

[2]J. F. Ziegler, *Helium Stopping Powers and Ranges in All Elements* (Pergamon, New York, 1978).

[3]H. H. Anderson and J. F. Ziegler, *Hydrogen Stopping Powers and Ranges in All Elements* (Pergamon, New York, 1977).

[4]P. Jung, J. Nucl. Mater. **117**, 70 (1983).

[5]R. Vassen, Diplomarbeit, Rheinisch-Westfälische Technische Hochschule Aachen, Germany, 1986.

[6]J. Odenthal, Diplomarbeit, Rheinisch-Westfälische Technische Hochschule Aachen, Germany, 1984.

[7]T. M. Buck, L. C. Feldman, and G. H. Wheatley, *Collisions in Solids I* (Plenum, New York, 1975), p. 331.

[8]C. F. Barnett, J. A. Ray, E. Ricci, and M. I. Wilker, Oak Ridge National Laboratory Report No. ORNL-5207 (unpublished).

[9]G. Duesing, Ph.D. thesis, Rheinisch-Westfälische Technische Hochschule Aachen, Germany, 1969.

[10]G. Burger, Ph.D. thesis, Technische Hochschule München, Germany, 1965.

[11]*Physik-Daten Nr. 5-20, Gases and Carbon in Metals, Pt. XX: Platinum Metals (2)* edited by H. Jehn, H. Speck, W. Hehn, E. Fromm, and G. Hörz (Fachinformationszentrum Energie-Physik-Mathematik G.m.b.H., Karlsruhe, 1982).

[12]A. S. Berger, D. Seidman, and R. W. Balluffi, Acta Metall. **21**, 123 (1973).

[13]C. Papastaikoudis, B. Lengeler, and W. Jäger, J. Phys. F **13**, 2257 (1983).

[14]M. C. Cadeville and C. Lerner, Philos. Mag. **33**, 801 (1976).

[15]J. B. Comly and J. L. Swartz, J. Appl. Phys. **42**, 1334 (1971).

[16]A. Gaber, Report, Kernforschungsanlage Jülich G.m.b.H., Report No. Jül-1860, 1983 (unpublished).

[17]W. Brandt, A. Ratkowski and R. H. Ritchie, Phys. Rev. Lett. **33**, 1325 (1974).

[18]W. Jäger, J. Microsc. Spectrosc. Electron **6**, 437 (1981).

[19]D. A. Thompson, Rad. Eff. **56**, 105 (1981).

[20]V. Sciani and P. Jung, Rad. Eff. **78**, 87 (1983).

[21]W. D. Wilson, C. L. Bisson, and M. I. Baskes, Phys. Rev. B **24**, 5616 (1981).

[22]E. Ligeon, R. Danielou, J. Fontenille, and R. Eymery, J. Appl. Phys. **59**, 108 (1986).

[23]D. S. Gemmell, J. Remillieux, J.-C. Poizat, M. J. Gaillard, R. E. Holland, and Z. Vager, Phys. Rev. Lett. **34**, 1420 (1975).

[24]C. Baker and H. K. Birnbaum, Acta. Metall. **21**, 865 (1973).

[25]J. F. Ziegler, J. P. Biersack, and U. Litmark, *Stopping and Range of Ions in Solids* (Pergamon, New York, 1985), Vol. 1.